Catalysis Today 149 (2010) 358–364

Contents lists available at ScienceDirect

Catalysis Today

journal homepage: www.elsevier.com/locate/cattod

Carbon xerogel supported noble metal catalysts for fine chemical applications

Bruno F. Machado [a], Helder T. Gomes [a,b], Philippe Serp [c], Philippe Kalck [c], José L. Figueiredo [a], Joaquim L. Faria [a,*]

[a] Laboratório de Catálise e Materiais (LCM), Laboratório Associado LSRE/LCM, Departamento de Engenharia Química, Faculdade de Engenharia, Universidade do Porto, Rua Dr. Roberto Frias s/n, 4200-465 Porto, Portugal

[b] Departamento de Tecnologia Química e Biológica, Escola Superior de Tecnologia e Gestão, Instituto Politécnico de Bragança, Campus de Santa Apolónia, 5300-857 Bragança, Portugal

[c] Laboratoire de Chimie de Coordination UPR CNRS 8241, École Nationale Supérieure d'Ingénieurs en Arts Chimiques et Technologiques, 118 route de Narbonne, 31077 Toulouse Cedex 4, France

ARTICLE INFO

Article history:
Available online 31 July 2009

Keywords:
Carbon xerogel
Platinum
Iridium
Ruthenium
Selective hydrogenation
Cinnamaldehyde

ABSTRACT

Carbon xerogels are mesoporous materials obtained upon pyrolysis of the dried gels resulting from polycondensation of resorcinol and formaldehyde. Treatment with nitric acid under severe conditions introduces high amounts of oxygen containing functional groups onto the surface of the material, leading however to the collapse of its porous structure. The resulting material is then used to support 1 wt.% Pt, Ir and Ru monometallic catalysts by wet impregnation using organometallic precursors. The catalysts are characterized by N_2 adsorption–desorption isotherms at 77 K, temperature programmed desorption coupled with mass spectrometry, scanning and transmission electron microscopy, and H_2 chemisorption. The liquid-phase selective hydrogenation of cinnamaldehyde to cinnamyl alcohol is used in order to assess the catalytic performance of the prepared materials. Pt and Ru catalysts are initially very selective towards the hydrogenation of the olefinic double bond, while Ir is mostly selective towards the carbonyl group. After a thermal post-reduction treatment at 973 K, selectivity towards cinnamyl alcohol is significantly improved regardless of the metal nature. The Pt catalyst exhibits the best behavior, a complete shift in C=C to C=O hydrogenation being detected. The improvement in selectivity is rationalized in terms of both an increase in metal particle size and a modification in the surface chemistry of the catalyst after the post-reduction treatment.

1. Introduction

Since the 1990s, resorcinol-formaldehyde organic gels have received considerable attention as carbon precursors due to their unique properties, such as high surface areas and controlled porous structures [1–3]. Starting from the first report by Pekala [4], research has been focused on achieving and controlling the degree of meso/macroporosity of these carbon materials and on modifying the synthesis procedures. From the reaction engineering point of view, when working either in the liquid- or gas-phase, the use of non-microporous materials is considered highly desirable in order to avoid internal mass-transfer limitations [5,6].

Three different types of carbon gels can be obtained depending on the solvent drying method [5,7]: aerogels (drying under supercritical CO_2), xerogels (drying at ambient temperature and pressure conditions) and cryogels (freeze drying). Depending on the pH and the dilution ratio of the starting resorcinol-formaldehyde precursor solution, these materials can present widely different textures [3,8–11]. Carbon xerogels (CXs) have been used as catalyst supports in fuel cells [1,12,13], using metals like Pt and Ru, but also as catalysts in advanced oxidation processes (AOPs), such as wet air oxidation [14,15], and in fine chemical applications [16,17].

Efficiency and environmental impact are pushing the use of heterogeneous catalysts for the synthesis of fine chemicals. Indeed, heterogeneous catalytic processes are always easier to handle than the homogeneous ones and lead to lower amounts of waste products, thus lowering environmental risks [18]. Research focused on chemo- and regio-selective catalytic hydrogenation of unsaturated compounds to produce fine chemicals is rapidly growing. In the past few years, considerable efforts have been devoted to the development of catalytic systems able to perform selective hydrogenation of the carbonyl function in α,β-unsaturated aldehydes [19–22]. The unsaturated alcohols are important intermediates in organic synthesis of fine chemicals for several industries such as flavor, fragrance, pharmaceutical and agrochemical. The formation of unsaturated alcohols in high yields, avoiding the use of toxic reducing agents such as metal hydrides,

* Corresponding author. Tel.: +351 225 081 645; fax: +351 225 081 449.
E-mail address: jlfaria@fe.up.pt (J.L. Faria).

0920-5861/$ – see front matter © 2009 Elsevier B.V. All rights reserved.
doi:10.1016/j.cattod.2009.06.016

commonly applied in preparative organic chemistry, is thus highly desirable [18,22,23]. Unfortunately, high selectivities towards these alcohols are difficult to achieve, since thermodynamics favors the hydrogenation of the C=C over the C=O bond by about 35 kJ mol^{-1} [24]. To increase selectivity, this thermodynamic constraint must be reduced by preferential adsorption of the carbonyl function at the catalyst surface.

It has been found that selectivity towards the allylic alcohol is highly dependent on the nature of the metal used. Metals such as Pt, Os, Ir, Pd, Rh and Ru, among others, have been studied, showing significant differences in activity and selectivity. Gallezot and Richard [22] reported that unpromoted Ir and Os catalysts are rather selective for unsaturated alcohol formation, while Pt, Ru and Co are moderately selective and Pd, Rh and Ni are non-selective.

In this work, the effect of high temperature activation of CX supported noble metal catalysts on their performances is studied, using the hydrogenation of cinnamaldehyde as model reaction.

2. Experimental

2.1. Support preparation

An aqueous organic gel was prepared by polycondensation of resorcinol with formaldehyde (1:2), adapting the procedure described by Job et al. [11]. Accordingly, 56.57 g of resorcinol (Aldrich, 99%) were added to 113 mL of deionised water in a glass flask. After complete dissolution, 82 mL of formaldehyde solution (Sigma, 37 wt.% in water, stabilized with 15 wt.% methanol) were also added. In order to achieve the 6.0 value for the initial pH of the precursor solution, sodium hydroxide solutions (5 and 10 M) were added dropwise under continuous stirring and pH monitoring. The precise control of this parameter was found to be determinant in the development of the meso/macroporous character of CX materials [11]. The gelation step was allowed to proceed at 358 K during 3 days, after which the gel displayed a dark red color. At this point, the consistency of the material allowed the sample to be shaped as desired (ground to small particles *ca.* 0.1 mm). The gel was further dried in oven from 333 to 423 K, defining a heating ramp of 20 K day^{-1} and maintaining the temperature of 423 K for 3 days. After drying, the gel was pyrolyzed at 1073 K under a nitrogen flow (100 cm^3 min^{-1}) in a tubular vertical furnace.

A liquid-phase treatment with boiling nitric acid (*ca.* 7 M) was used in order to introduce oxygen containing functional groups onto the surface of the previously prepared CX material. The material was then thoroughly washed with water until neutrality of the rinsing waters and dried in an oven for 2 days at 393 K.

2.2. Catalyst preparation

$[Pt(CH_3)_2(COD)]$, $[Ir(\mu\text{-}SC(CH_3)_3)(CO)_2]_2$ and [Ru(COD)(COT)] were used, respectively, as metal precursors in the preparation of Pt, Ir and Ru catalysts supported on the carbon xerogel treated with nitric acid. These precursors were used successfully in previous works [25–27]. One of their main advantages is that they can be easily anchored to the oxygen containing functional groups on the surface of carbon materials, due to their organic functionalities, thus allowing metal deposition near theoretical values and maximum dispersion. In addition, the selected organometallic precursors are characterized by a clean decomposition upon reduction and calcination treatments.

The platinum precursor was synthesized by a procedure described in detail elsewhere [28]. The first step involved the preparation of the intermediate $[PtI_2(COD)]$, by addition of 1,5-cyclooctadiene (commonly designated as COD, C_8H_{12}, Aldrich, 99%) to platinum(II) iodide (PtI_2, Strem Chemicals, 99%). Further addition of diethyl ether ($C_4H_{10}O$), methyllithium solution (CH_3Li, Fluka, 5%) and sodium sulphate (Na_2SO_4, Acros Organics, 99%) was necessary to prepare the final complex $[Pt(CH_3)_2(COD)]$. The iridium precursor was also synthesized following a procedure described elsewhere [29], which involves the addition of calculated amounts of iridium (III/IV) iodide ($IrI_{3,4}$, Johnson Matthey, 31.8%), N,N-dimethylformamide (C_3H_7NO, Acros Organics, 99%), distilled water and 2-methyl-2-propanethiol ($((CH_3)_3CSH$, Acros Organics, 99%). The ruthenium precursor, [Ru(COD)(COT)] (COT = 1,3,5-cyclooctatriene, C_8H_{10}, NanoMePS), was used as received.

All the catalysts were prepared by wet impregnation. The desired amounts of metal precursor, calculated in order to introduce 1 wt.% of metal, carbon xerogel and *n*-hexane (solvent) were placed in a Schlenk tube under argon atmosphere. After being stirred for 2 days at 318 K the catalysts were filtered and dried overnight (393 K). Prior to reaction Pt and Ru catalysts were calcined at 673 K (N_2, 4 h) and reduced at 623 K (H_2, 2 h). The Ir catalyst was calcined (N_2, 4 h) and reduced (H_2, 2 h) at a different temperature (773 K) in order to remove the sulfur introduced by the precursor [29]. After the reduction step all the catalysts were flushed again with nitrogen for 30 min to remove physisorbed hydrogen. These catalysts will be referred here as Pt/CX, Ir/CX and Ru/CX. A post-reduction treatment (PRT) under nitrogen at 973 K was also performed to remove excess oxygen containing surface groups, and the corresponding catalysts are designated as Pt/CX973, Ir/CX973 and Ru/CX973.

2.3. Catalyst characterization

Textural characterization was based on the analysis of the N_2 adsorption–desorption isotherms, determined at 77 K with a Coulter Omnisorp 100CX apparatus. Specific BET surface areas (S_{BET}) were calculated, as well as the micropore volumes (V_{MIC}) and the non-microporous surface areas (mainly mesoporous, S_{MES}) determined by the *t*-method, using the standard isotherm for carbon materials proposed by Rodriguez-Reinoso et al. [30].

TPD spectra were obtained with a fully automated AMI-200 Catalyst Characterization Instrument (Altamira Instruments), equipped with a quadrupole mass spectrometer (Dymaxion 200 amu, Ametek). The sample (0.10 g) was placed in a U-shaped quartz tube located inside an electrical furnace and heated at 5 K min^{-1} to 1373 K using a constant flow rate of helium (25 cm^3 min^{-1}, STP). The amounts of CO and CO_2 released during the thermal analysis were calibrated at the end of each analysis. This allowed the identification and quantification of the different types of oxygen containing functional groups at the materials surface by analysis of the corresponding TPD spectra using the peak assignment and deconvolution procedures described by Figueiredo et al. [31,32].

Surface analysis for topographical and analytical characterization was carried out by scanning electron microscopy (SEM) with a JEOL JSM-6301F (15 keV) electron microscope equipped with an OXFORD INCA ENERGY 350 energy dispersive X-ray spectroscopy (EDS) system. The sample powders were mounted on a double-sided adhesive tape and observed at different magnifications under two different detection modes, secondary and back-scattered electrons.

H_2 chemisorption was performed at room temperature in a U-shaped tubular quartz reactor after a thermal treatment (2 cm^3 min^{-1} H_2 and 28 cm^3 min^{-1} He for 2 h and 30 cm^3 min^{-1} He for another 2 h at 773 K) to remove possible contaminant species from the catalyst surface. Pulses of H_2 were injected through a calibrated loop into the sample at regular time intervals until the area of the recorded peaks became constant. The amounts of H_2 chemisorbed were calculated from the areas of the resultant H_2 peaks, monitored with a SPECTRAMASS Dataquad quadrupole

mass spectrometer. Assuming the formation of spherical particles and a surface concentration of 1.25×10^{19} at m^{-2} for Pt, 1.30×10^{19} at m^{-2} for Ir and 1.63×10^{19} at m^{-2} for Ru it was possible to estimate the mean particle diameter of the metals, based on the observed metal dispersions (H/M, M = Pt, Ir or Ru) [33]:

$$d_{Pt}[nm] = \frac{1.133}{(H/Pt)} \quad (1)$$

$$d_{Ir}[nm] = \frac{1.099}{(H/Ir)} \quad (2)$$

$$d_{Ru}[nm] = \frac{1.318}{(H/Ru)} \quad (3)$$

Transmission electron microscopy (TEM) observations were made with a LEO 906 E from LEICA (120 keV voltage). The samples were dispersed in ethanol, sonicated and collected on a carbon-coated copper TEM grid. The mean particle sizes were determined by direct inspection of the micrographs and evaluated according to the average diameters (Eq. (4)) or the surface weighed average diameters (Eq. (5)) [34].

$$d = \frac{\Sigma n_i d_i}{N} \quad (4)$$

$$d = \frac{\Sigma n_i d_i^3}{\Sigma n_i d_i^2} \quad (5)$$

2.4. Catalytic hydrogenation

Hydrogenation of cinnamaldehyde was carried out in a 100 mL well-stirred stainless steel reactor. The reaction mixture contained *n*-heptane (Aldrich, 99%), cinnamaldehyde (Fluka, 98%), decane (Fluka, 98%, as internal standard for gas chromatography) and 0.2 g of catalyst. When the reaction was performed with the catalysts subjected to post-reduction treatment (M/CX973, M = Pt, Ir or Ru), the PRT procedure described in Section 2.2 was carried out on the previous day and extended, under inert atmosphere at room temperature, until moments before starting the reaction. Nitrogen was bubbled through the solution several times to remove traces of dissolved oxygen. The reactor was then pressurized with hydrogen (3 bar) in order to purge the nitrogen. Finally, the temperature was set at 363 K and the reactor pressurized with hydrogen to the desired 10 bar immediately before starting the reaction. Small aliquots were analyzed at different reaction times to monitor product distribution. The results of the reaction runs were analyzed in terms of reactant conversion, product selectivity and turn-over frequency (TOF) in an identical way to that described elsewhere [25].

The analysis was performed with a DANI GC-1000 gas chromatograph, equipped with a split/splitless injector, a capillary column (WCOT Fused Silica 30 m, 0.32 mm i.d., coated with CP-Sil 8 CB low bleed/MS 1 μm film) and a flame ionization detector.

3. Results and discussion

3.1. Support characterization

TPD experiments performed on CX before (CX-orig.) and after ($CX\text{-}HNO_3$) nitric acid treatment (Fig. 1) clearly show the difference in the amount of surface groups in both samples. Depending on the type of treatment performed, carbon materials often develop large amounts of surface groups, namely carboxylic acids (released by TPD at 573 K), anhydrides (800 K), phenols (950 K), lactones (1000 K) and carbonyl/quinones (1100 K) [32].

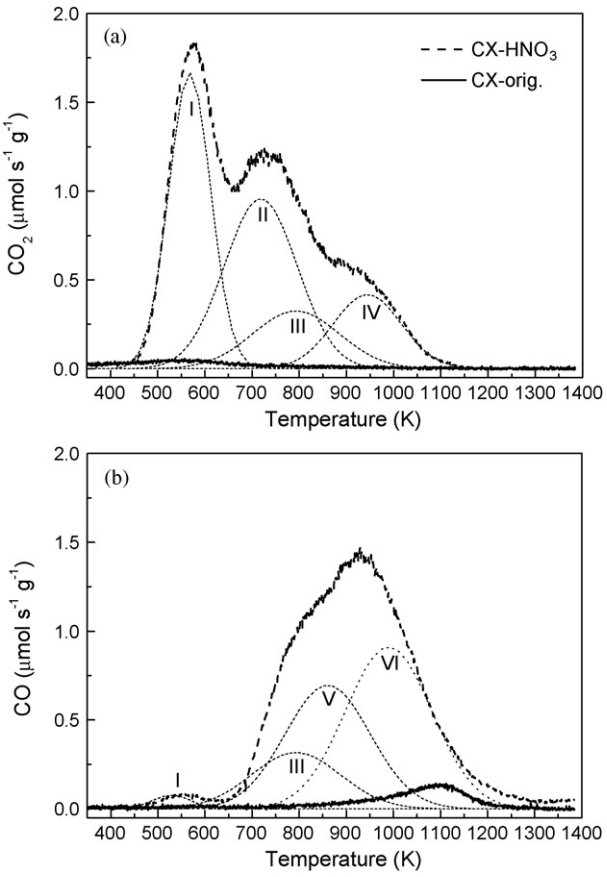

Fig. 1. TPD spectra of CX before (CX-orig.) and after ($CX\text{-}HNO_3$) nitric acid treatment: (a) CO_2 and (b) CO evolution.

Surface group identification can be carried out by TPD deconvolution, a common technique used within our group. Details regarding curve fitting can be found elsewhere [31,32]. Following the described procedures it was possible to identify high amounts of carboxylic acid groups (I and II, 6815 and 2222 μmol g^{-1}, respectively in Fig. 1), phenols (V, 1891 μmol g^{-1}) and carbonyl/quinones (VI, 2507 μmol g^{-1}), and lower amounts of anhydrides (III, 900 μmol g^{-1}) and lactones (IV, 906 μmol g^{-1}) in $CX\text{-}HNO_3$. These surface groups, mainly carboxylic acids, act as anchoring sites for metal particles and are able to increase metal dispersion in carbon material supports. For example, it has been recently evidenced that finely dispersed Pt clusters bind to MWCNT surface via bonding with ionic form of carboxylate –COO(Pt) [35].

No deconvolution was carried out for the untreated CX sample due to the very low amounts of CO and CO_2 desorbed. However, an indication of the material surface acidity can be provided by the CO/CO_2 ratio, since the most acidic groups are released as CO_2, while the less acidic and basic groups are released as CO. A strong increase in acidity was observed upon nitric acid activation since CO/CO_2 decreased from 1.9 to 0.9. Although the concentration of CO increases from 391 to 5468 μmol g^{-1}, that of CO_2 increases from 205 to 6281 μmol g^{-1}. The effect of the oxidation with nitric acid on the surface properties of CX can be observed in Table 1.

The type and amount of surface groups introduced depends on the concentration of the activating agent used (gas- or liquid-phase). Usually, as the severity of the treatment increases, it is more likely that the structure suffers some form of degradation. To study the effect of the liquid-phase activation over the texture of the material, N_2 adsorption–desorption isotherms at 77 K were performed. Both samples produced type IV adsorption isotherms

Table 1
Textural properties of CX before (CX-orig.) and after (CX-HNO_3) nitric acid treatment and corresponding amounts of CO and CO_2 released by TPD.

Sample	S_{BET} (± 5 m^2 g^{-1})	S_{MES} (± 5 m^2 g^{-1})	V_{MIC} (± 0.01 cm^3 g^{-1})	CO (± 20 μmol g^{-1})	CO_2 (± 20 μmol g^{-1})	CO/CO_2
CX-orig.	627	180	0.18	391	205	1.9
CX-HNO_3	20	6	0.01	5468	6281	0.9

with H1 hysteresis loops characteristic of mesoporous materials [36]. However, the amounts of adsorbed nitrogen were quite different, a drastic decrease being observed with CX-HNO_3. The reason why this material underwent such a strong surface area reduction has to do with the severity of the nitric acid treatment, which caused the porous structure to practically disappear as shown by the calculated textural properties (Table 1). There is a 18-fold reduction in micropore volume after the nitric acid functionalization, the average pore size for the untreated CX being *ca.* 10 nm, based on the N_2 desorption isotherm at 77 K.

SEM analyses were performed in order to examine the modifications occurring in the carbon structure after nitric acid oxidation. A typical structure for mesoporous carbon xerogels can be observed in CX before nitric acid treatment (Fig. 2a), while a much smoother arrangement of the surface is present in the material CX-HNO_3 (Fig. 2b), evidencing the collapse of the structure. Comparing the CX material against other carbon materials, namely multi-walled carbon nanotubes or carbon nanofibers where a high degree of functionalization can be achieved without damaging the main structure [25,37], it can be observed that the carbon xerogel is not so stable under strong liquid-phase oxidative conditions. This limitation of CX can be in part solved by using a Soxhlet extractor to treat the xerogels [38] under milder acidic conditions. A surface area decrease is observed to a minor extent (4–6%), but the degree of functionalization is much lower than that obtained with the more severe treatment. Accordingly, the amount of surface groups released as CO and CO_2 reported in this manuscript is, respectively, *ca.* 2.5 and 5 times higher than that observed with the Soxhlet-treated sample. In addition, TPD spectra in both works present similar profiles, i.e. the same type of surface groups were present in both cases.

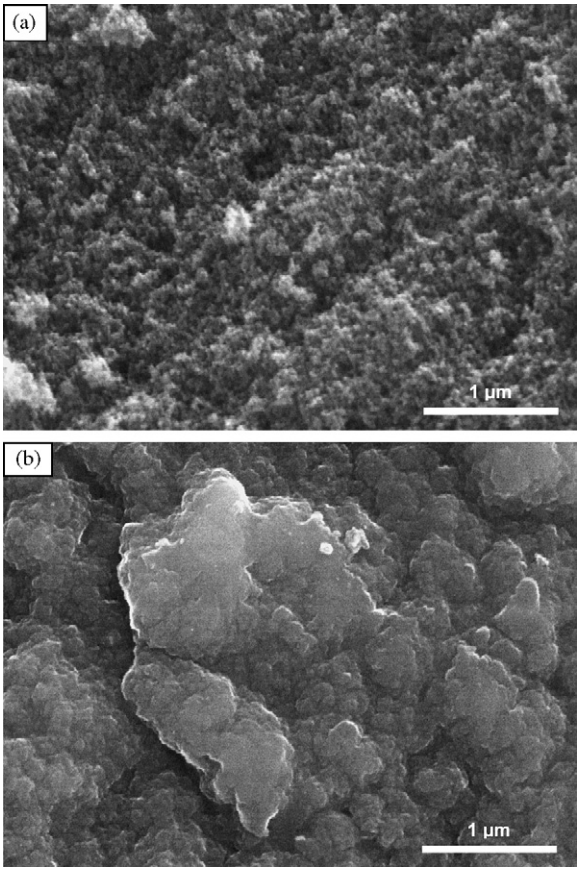

Fig. 2. SEM micrographs of CX (a) before and (b) after nitric acid treatment.

Hence, a compromise regarding the severity of the treatment has to be taken into account if the carbon xerogel pore structure is to be preserved while introducing large amounts of surface groups. Regarding the impact of the pore texture degradation on the mass transport in catalytic reactions, since the material texture changes from a mesoporous character to a macro-nonporous character, it is expected that diffusional limitations, that may eventually be present when using the original material, will be absent when using the oxidized material, with obvious advantages from the engineering point of view.

3.2. Metal-phase characterization

The mean metal particle size was determined from TEM analysis, showing Pt particles around 3 nm in the Pt/CX catalyst (Fig. 3), and Ir and Ru ones with *ca.* 2 nm in the Ir/CX and Ru/CX catalysts (Table 2). After the PRT at 973 K, an increase in the metal particle sizes was observed to varying extents for all catalysts, as a result of sintering phenomena. The Pt catalyst displayed the highest increase, yielding particles with *ca.* 7 nm, while the extent of the sintering effects for the Ir and Ru catalysts was somewhat lower. The surface weighed average diameters obtained from TEM observations are somewhat larger than those obtained by H_2 chemisorption measurements (Table 2). In fact, since chemisorption measurements depend on surface analysis, the values obtained by this technique should be in fair agreement with the presented surface weighed average diameter.

With the exception of Ru/CX973, all the remaining catalysts evidenced smaller particle sizes determined by H_2 chemisorption when compared to TEM analysis. A possible explanation for this observation could be related to a spill-over phenomenon, typically observed in carbon materials [39].

In spite of the low surface area of CX treated with nitric acid, high metal dispersions were initially observed regardless of the metal nature. There are two main factors that can help explain the obtained dispersion values: low metal load present (perhaps the most important) and the oxygenated groups on the surface of the carbon material. The importance of the surface groups was previously reported and related to their capacity to act as anchoring sites for the metal particles during the deposition process [25].

The larger extent of sintering observed in the Pt/CX catalyst subjected to PRT was expected, considering the Hüttig ($T_H \approx 1/3T_f$) and Tammann ($T_T \approx 1/2T_f$) temperatures (Table 3), where T_f represents the metal melting point. These values give an indication of the temperatures at which sintering starts to occur [40] and are well within the range of the post-reduction treatment at 973 K for Pt catalysts. Ir and Ru catalysts were found to be much more stable over the CX surface, as smaller variations regarding the initial metal particle size were observed. Nevertheless, it was still possible to prepare well dispersed and somewhat thermally stable catalysts, by treating the surface of the support accordingly.

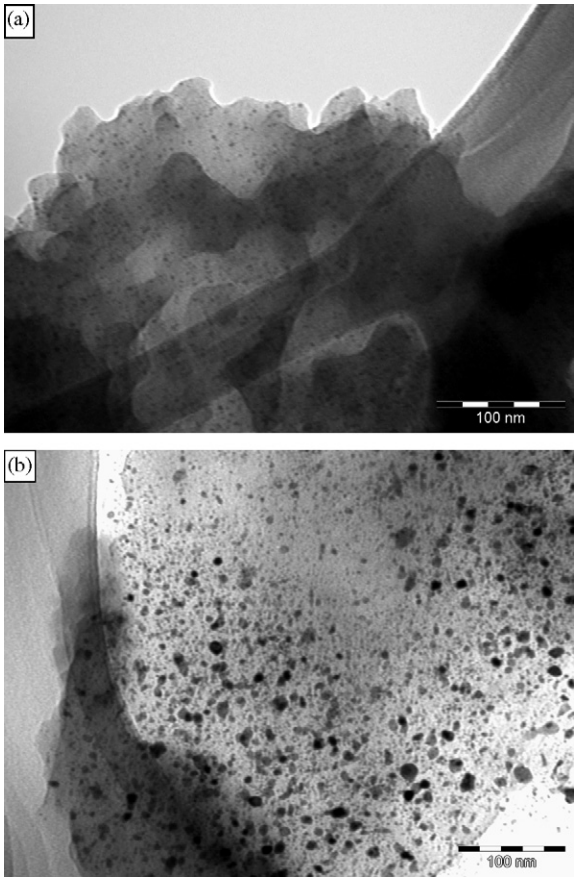

Fig. 3. TEM micrographs of (a) Pt/CX and (b) Pt/CX973.

Table 2
Mean particle size (d_{Me}) determined by H_2 chemisorption and TEM analysis of CX supported Pt, Ir and Ru catalysts.

Catalyst	d_{Me} (±0.1 nm)		
	H_2 chemisorption	TEM (average diameter)[a]	TEM (surface weighed)[b]
Pt/CX	2.9	3.3	3.6
Pt/CX973	4.2	6.8	7.9
Ir/CX	1.8	2.2	2.5
Ir/CX973	2.7	3.2	3.4
Ru/CX	1.4	1.8	2.3
Ru/CX973	2.5	2.3	2.9

[a] According to Eq. (4).
[b] According to Eq. (5).

Table 3
Hüttig and Tammann temperatures.

Metal	T_f (K)	T_H (K)	T_T (K)
Pt	2043	681	1022
Ir	2723	908	1362
Ru	2523	841	1262

3.3. Selective hydrogenation

Fig. 4 shows the reaction scheme proposed involving the main compounds detected in the selective hydrogenation of cinnamaldehyde (CAL) with CX supported catalysts. The hydrogenation of CAL proceeds via the parallel and consecutive reduction of different functional groups i.e., C=C and C=O bonds. Typically, a mixture of the desired cinnamyl alcohol (COL) together with hydrocinnamaldehyde (HCAL) and hydrocinnamyl alcohol (HCOL) is obtained. A number of side-products that involve the loss of the hydroxyl group were also detected regardless of the metal nature, mainly significant amounts of β-methylstyrene (MS) and 1-propylbenzene (PB). PB can be obtained either by hydrogenation of MS or by hydrogenolysis of HCOL.

The catalytic results from the liquid-phase hydrogenation of cinnamaldehyde with CX supported Pt, Ir and Ru catalysts are gathered in Table 4, more specifically the TOF based on the conversion of cinnamaldehyde and the selectivities towards cinnamyl alcohol (S_{COL}), hydrocinnamaldehyde (S_{HCAL}) and hydrocinnamyl alcohol (S_{HCOL}), at 50% conversion of CAL.

Pt/CX and Ru/CX catalysts were relatively non-selective towards COL (20% and 5%, respectively), whereas the Ir/CX catalyst evidenced a high selectivity towards COL (57%). A possible reason for this behavior can be associated with the use of a higher temperature (773 K) during the calcination step (necessary to remove sulfur from the Ir precursor), allowing for a partial removal of the surface groups when compared with Pt/CX and Ru/CX catalysts (whose calcinations were performed at 673 K).

In a previous work, a high temperature post-reduction treatment applied to multi-walled carbon nanotubes supported Pt catalysts [25] was found to bring enormous benefits to the catalyst performance. This improvement was related to the removal of most of the surface groups found at the catalyst surface, while inducing a sintering effect of the metal particles. The results here presented with CX supported catalysts, confirm the beneficial effect of this thermal treatment over both TOF and selectivity to COL. In all cases, a significant improvement could be observed in the production of COL. The most outstanding result was obtained when using Pt, where a complete shift in HCAL to COL selectivity was noticed. The product distribution throughout the reaction using the Pt/CX973 catalysts is shown in Fig. 5 as a typical example.

The enhancement observed after the PRT in the Ir catalyst was not as pronounced as that observed for the Pt catalyst, but nevertheless a selectivity of 65% was obtained. The Ru/CX catalyst was quite selective towards the usually undesired HCAL, with a selectivity of 65% being observed. After the PRT an increase in COL selectivity from 5% to 32% was observed. The influence of the Ru particle size supported on activated carbon was studied by Galvagno et al. [41] in the same hydrogenation reaction. They observed that the selectivity to cinnamyl alcohol increased with Ru particle size to values as high as 61%, when particles *ca.* 17 nm were used. In our case, since the Ru particle size remained practically unchanged, the improved selectivity could also be due to the removal of the surface groups. This modification of the catalyst surface is thought to enable the preferential adsorption of the C=O rather than the C=C bond.

Gallezot and Richard showed that there is a correspondence between the nature of active metals, their size and selectivity [22]. It has been shown [42] that metal selectivities can be explained in terms of the different radial expansion of their d bands (the larger the band, the stronger the four-electron repulsive interactions with the C=C bond and the lower the probability of its adsorption); the influence of the particle size is explained in terms of a steric effect, where the planar cinnamaldehyde molecule cannot adsorb parallel to a flat metal surface due to the steric repulsion of the aromatic ring (the selectivity improvement is due to the lower probability of activation of the C=C bond rather than to an increased activation of the C=O). Thus, Ir catalysts are more selective than Pt and Ru ones, considering similar particle sizes, and, for each metal, selectivities were also observed to increase with increasing particle size. In this work, the higher selectivity exhibited by the Pt catalyst can also be related to its particle size. The usually less selective character of the Pt catalyst is somewhat surpassed by the increased metal particle size, regarding that observed for Ir particles.

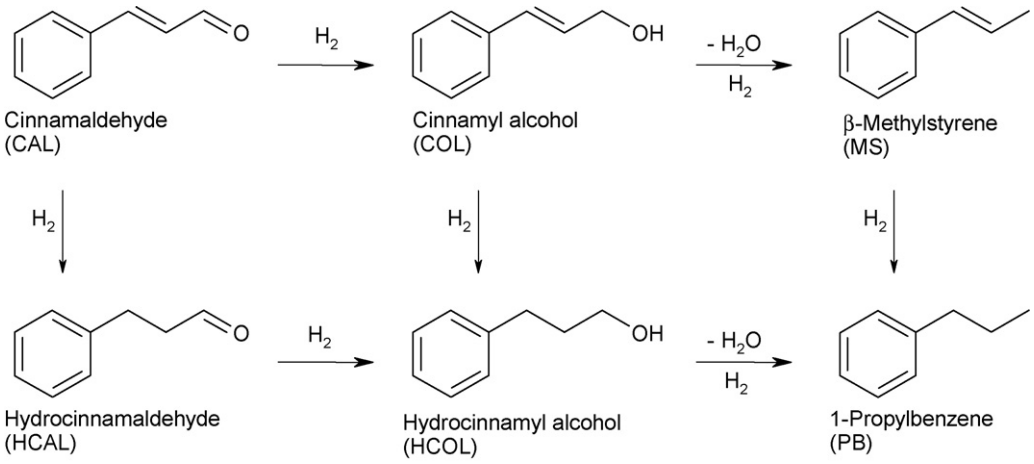

Fig. 4. Reaction scheme proposed for the selective hydrogenation of cinnamaldehyde using CX supported Pt, Ir and Ru catalysts.

Table 4
Catalytic results obtained in the hydrogenation of cinnamaldehyde at 363 K and 10 bar, using CX supported catalysts (selectivities measured at 50% conversion).

Catalyst	TOF (±0.1 s^{-1})	S_{COL} (±1%)	S_{HCAL} (±1%)	S_{HCOL} (±1%)
Pt/CX	1.4	20	39	18
Pt/CX973	3.8	73	7	6
Ir/CX	2.1	57	20	9
Ir/CX973	2.4	65	20	8
Ru/CX	0.7	5	65	8
Ru/CX973	0.9	32	42	14

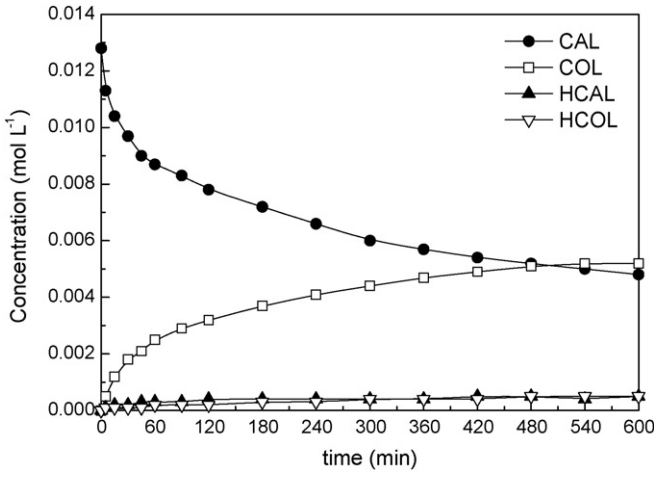

Fig. 5. Product distribution for the selective hydrogenation of cinnamaldehyde using the Pt/CX973 catalyst.

In summary, the preferential hydrogenation of the carbonyl bond in the studied catalysts is explained based on a combined effect of both metal particle size increase and surface chemistry of the catalyst, through the removal of surface groups.

4. Conclusions

A severe treatment with nitric acid created large amounts of oxygen containing functional groups at the surface of a carbon xerogel material, however compromising its original porous structure, yielding a practically non-porous material, with a low surface area.

Despite the loss of the textural properties of the carbon xerogel treated with nitric acid, catalysts prepared supporting Pt, Ir and Ru from organometallic precursors by wet impregnation presented small metal particles: 3 nm for Pt and around 2 nm for Ir and Ru.

A post-reduction thermal treatment of the catalysts at 973 K led to various degrees of sintering, mainly dependent on the nature of the active metal-phase.

The same thermal treatment also influenced the catalyst performance in the liquid-phase hydrogenation of cinnamaldehyde, pushing the selectivity towards cinnamyl alcohol, regardless of the metal nature. This increase in selectivity upon the post-reduction treatment is explained by the combined effect of both metal particle size increase, due to sintering, and the modification of the catalysts surface chemistry, which enhances the adsorption of the carbonyl group.

The Pt catalyst after the post-reduction treatment was found to be the most selective towards the preferential hydrogenation of the carbonyl group, followed by the Ir and Ru catalysts.

Acknowledgements

This research was carried out under the projects POCTI/58252/EQU/2004, REEQ/1106/EQU/2005, FEDER/POCI/2010 and SFRH/BD/16565/2004, approved by the Fundação para a Ciência e a Tecnologia (FCT) and co-supported by FEDER.

References

[1] C. Arbizzani, S. Beninati, E. Manferrari, F. Soavi, M. Mastragostino, J. Power Sources 172 (2007) 578.
[2] P.V. Samant, F. Gonçalves, M.M.A. Freitas, M.F.R. Pereira, J.L. Figueiredo, Carbon 42 (2004) 1321.
[3] C. Lin, J.A. Ritter, Carbon 35 (1997) 1271.
[4] R.W. Pekala, J. Mater. Sci. 24 (1989) 3221.
[5] N. Job, A. Théry, R. Pirard, J. Marien, L. Kocon, J.-N. Rouzaud, F. Béguin, J.-P. Pirard, Carbon 43 (2005) 2481.
[6] N. Job, B. Heinrichs, S. Lambert, J.-P. Pirard, J.-F. Colomer, B. Vertruyen, J. Marien, AIChE J. 52 (2006) 2663.
[7] T. Yamamoto, T. Nishimura, T. Suzuki, H. Tamon, Dry Technol. 19 (2001) 1319.
[8] S.A. Al-Muhtaseb, J.A. Ritter, Adv. Mater. 15 (2003) 101.
[9] C. Moreno-Castilla, F.J. Maldonado-Hodar, Carbon 43 (2005) 455.
[10] B. Babic, B. Kaluderovic, L. Vracar, N. Krstajic, Carbon 42 (2004) 2617.
[11] N. Job, R. Pirard, J. Marien, J.P. Pirard, Carbon 42 (2004) 619.
[12] N. Job, J. Marie, S. Lambert, S. Berthon-Fabry, P. Achard, Energy Convers. Manage. 49 (2008) 2461.
[13] J.L. Figueiredo, M.F.R. Pereira, P. Serp, P. Kalck, P.V. Samant, J.B. Fernandes, Carbon 44 (2006) 2516.
[14] H.T. Gomes, B.F. Machado, A. Ribeiro, I. Moreira, M. Rosário, A.M.T. Silva, J.L. Figueiredo, J.L. Faria, J. Hazard. Mater. 159 (2008) 420.
[15] Â.C. Apolinário, A.M.T. Silva, B.F. Machado, H.T. Gomes, P.P. Araújo, J.L. Figueiredo, J.L. Faria, Appl. Catal. B 84 (2008) 75.
[16] P.V. Samant, M.F.R. Pereira, J.L. Figueiredo, Catal. Today 102–103 (2005) 183.
[17] N. Mahata, F. Gonçalves, M.F.R. Pereira, J.L. Figueiredo, Appl. Catal. A 339 (2008) 159.
[18] F. Ammari, J. Lamotte, R. Touroude, J. Catal. 221 (2004) 32.

[19] P. Maki-Arvela, J. Hajek, T. Salmi, D.Y. Murzin, Appl. Catal. A 292 (2005) 1.
[20] P. Claus, Top. Catal. 5 (1998) 51.
[21] P. Kluson, L. Cerveny, Appl. Catal. A 128 (1995) 13.
[22] P. Gallezot, D. Richard, Catal. Rev.-Sci. Eng. 40 (1998) 81.
[23] K. Liberkova, R. Touroude, J. Mol. Catal. A: Chem. 180 (2002) 221.
[24] C. Mohr, P. Claus, Sci. Prog. 84 (2001) 311.
[25] A. Solhy, B.F. Machado, J. Beausoleil, Y. Kihn, F. Gonçalves, M.F.R. Pereira, J.J.M. Órfão, J.L. Figueiredo, J.L. Faria, P. Serp, Carbon 46 (2008) 1194.
[26] J. Garcia, H.T. Gomes, P. Serp, P. Kalck, J.L. Figueiredo, J.L. Faria, Carbon 44 (2006) 2384.
[27] H.T. Gomes, J.L. Figueiredo, J.L. Faria, P. Serp, P. Kalck, J. Mol. Catal. A: Chem. 182–183 (2002) 47.
[28] H.C. Clark, L.E. Manzer, J. Organomet. Chem. 59 (1973) 411.
[29] P. Serp, R. Feurer, P. Kalck, H. Gomes, J.L. Faria, J.L. Figueiredo, Chem. Vapour Depos. 7 (2001) 59.
[30] F. Rodriguez-Reinoso, J.M. Martin-Martinez, C. Prado-Burguete, B. McEnaney, J. Phys. Chem. 91 (1987) 515.
[31] J.L. Figueiredo, M.F.R. Pereira, M.M.A. Freitas, J.J.M. Órfão, Carbon 37 (1999) 1379.
[32] J.L. Figueiredo, M.F.R. Pereira, M.M.A. Freitas, J.J.M. Órfão, Ind. Eng. Chem. Res. 46 (2007) 4110.
[33] J.J.F. Scholten, A.P. Pijpers, A.M.L. Hustings, Catal. Rev.-Sci. Eng. 27 (1985) 151.
[34] G. Bergeret, P. Gallezot, in: G. Ertl, H. Knözinger, J. Weitkamp (Eds.), Handbook of Heterogeneous Catalysis, vol. 2, Wiley-VCH, Weinheim, 1997, p. 439.
[35] R.V. Hull, L. Li, Y. Xing, C.C. Chusuei, Chem. Mater. 18 (2006) (1780).
[36] K.S.W. Sing, D.H. Everett, R.A.W. Haul, L. Moscou, R.A. Pierotti, J. Rouquerol, T. Siemieniewska, Pure Appl. Chem. 57 (1985) 603.
[37] P. Serp, M. Corrias, P. Kalck, Appl. Catal. A 253 (2003) 337.
[38] N. Mahata, M.F.R. Pereira, F. Suarez-Garcia, A. Martinez-Alonso, J.M.D. Tascon, J. Figueiredo, J. Colloid Interface Sci. 324 (2008) 150.
[39] F. Rodríguez-Reinoso, I. Rodríguez-Ramos, C. Moreno-Castilla, A. Guerrero-Ruiz, J.D. López-González, J. Catal. 99 (1986) 171.
[40] J.L. Figueiredo (Ed.), Progress in Catalyst Deactivation, Martinus Nijhoff Publishers, Dordrecht, The Netherlands, 1982.
[41] S. Galvagno, G. Capannelli, G. Neri, A. Donato, R. Pietropaolo, J. Mol. Catal. 64 (1991) p237.
[42] F. Delbecq, P. Sautet, J. Catal. 152 (1995) 217.